applied sciences

MDPI

Article

Phase Behavior of Fluid Composition in Coalbed Methane Wells Pre- and Post-Workover: An Examination of the Panzhuang Block, Qinshui Basin, Shanxi, China

Qingwei Wang [1,*,†], Qiang Yan [2,3,*,†], Yan Zhang [2,3], Xiafan Xing [1] and Cailian Hao [2,3]

[1] College of Geosciences and Engineering, North China University of Water Resources and Electric Power, Jinshui East Road No. 136, Zhengzhou 450045, China
[2] Institute of Mineral Resources, Chinese Academy of Geological Sciences, Beijing 100037, China
[3] Research Center for Strategy of Global Mineral Resources, Chinese Academy of Geological Sciences, Beijing 100037, China
* Correspondence: qingweiwang@126.com (Q.W.); cagsyq@163.com (Q.Y.)
† These authors contributed equally to this work.

Abstract: Workover operations significantly impact the service life and gas production capacity of coalbed methane (CBM) wells and are crucial for optimizing resource exploitation. To investigate workover operations' impact on coal seam reservoirs, the authors designed a series of experiments and obtained the following results: (1) The workover operation induced a phase transition in the solid-liquid composition produced by the CBM well, indicating changes in the coal reservoir's internal structure. (2) During the stable production stage before and after the workover, the proportion of Na^+, Cl^-, Ca^{2+}, and Total Dissolved Solids (TDS) in the water samples showed a downward trend as a whole, while the HCO_3^-; after the workover, the Na^+, Cl^-, Ca^{2+}, and TDS all increased suddenly, while the HCO_3^- decreased. (3) While inorganic minerals predominated in the precipitation material during the stable production stage pre-workover, their proportion decreased post-workover, with a noticeable shift in their qualitative composition. (4) It is an indisputable fact that workover operations cause physical and chemical damage to coal seam reservoirs. During workover operation, how to avoid damage and conduct benign reconstruction to the reservoir will be the direction of our future efforts. The experimental results provide valuable insights that can guide the optimization of CBM workover operations and inform the strategic planning of subsequent drainage activities.

Keywords: coalbed methane; workover operation; fluid composition; stage change; coal reservoir

Citation: Wang, Q.; Yan, Q.; Zhang, Y.; Xing, X.; Hao, C. Phase Behavior of Fluid Composition in Coalbed Methane Wells Pre- and Post-Workover: An Examination of the Panzhuang Block, Qinshui Basin, Shanxi, China. *Appl. Sci.* **2024**, *14*, 7207. https://doi.org/10.3390/app14167207

Academic Editor: Keyu Liu

Received: 11 July 2024
Revised: 4 August 2024
Accepted: 13 August 2024
Published: 16 August 2024

1. Introduction

As of the end of 2020, China had 12,880 CBM production wells [1]. As the number of CBM production wells increases, so do the instances of drainage failures [2–4]. To restore normal production, workover operations have become increasingly important for CBM development [1,4,5]. However, these workover operations always cause damage to coal reservoirs to a certain extent [6–10]. This damage manifests as microscopic changes in the coal reservoir, further deteriorating its permeability [8,9]. Some scholars have posited that hydrodynamic conditions reflect changes in reservoir pressure states, influencing methane retention and dissipation, and also impact hydrophilic minerals and the migration of microscopic particles or molecules within the coal reservoir [8,11–16]. On one hand, the flow of groundwater carrying dissolved methane in coal seams stimulates exchange between free and adsorbed methane, resulting in increased methane entrainment during its continuous migration [8,14,17,18]. On the other hand, water flow within the coal reservoir can alter its original chemical properties, including pH value, TDS, and ionic composition [2,8,19,20]. It is widely accepted that the chemical composition of the produced water, being a closed system, remains relatively stable within a specific range in the

absence of external interference, such as well workovers [11,14,15,19]. During the workover process, multiple flushes can induce changes in the hydrodynamic field; thus, changes in water chemistry directly respond to alterations in the hydrodynamic field [21–23]. In CBM production, water and methane are generated together [2,4,24]. The water can be categorized into three types: fracturing fluid-contaminated water, formation water, and polluted surface water [25,26]. Studying the changes in the reservoir's internal structure due to CBM well workovers could analyze the changes in the composition of produced fluids before and after workover, a factor that has received little attention.

In China, the Qinshui Basin represents the largest commercial development area for CBM, with an estimated resource of 8.3 trillion cubic meters (m^3) of CBM, indicating significant reserves [27]. Utilizing production data from CBM wells in the Panzhuang block of the Qinshui Basin, the authors' research focuses on how workover operations impact the coal reservoir's internal structure. This research aims to offer insights and guidance for optimizing future CBM production strategies.

2. Geological Background

The selected site is located in the Qinshui Basin, situated in the central and southern parts of Shanxi Province, and its tectonic structure belongs to the Neo-Caxia tectonic system. A monoclinic structure dominates the entire basin, resulting in an overall structural orientation of NNE (Figure 1A) [28–30]. Within the southern Qinshui Basin, the Indosinian tectonic movement produced a SN-trending horizontal compressive stress field. However, this movement had minimal impact, leaving behind scant tectonic evidence [29,31]. In the Yanshanian period, near-horizontal compression of the NW-SE-trending stress field led to the formation of NNE-NE-trending secondary fold structures. These structures emerged as the primary gas-controlling configurations. Consequently, the gas-rich belt located in the southeast of the Qinshui Basin aligns in the NNE direction, following the axis of the secondary syncline [28,32]. Marked by a NW-SE-trending near-horizontal extensional stress field, the Himalayan tectonic movement led to the formation of small-scale, near-SN-trending secondary folds. These folds often represent the local centers of CBM gas richness [30,32].

The Qinshui Basin's primary coal-bearing strata comprise the Taiyuan and Shanxi Formations. These formations host over 10 mineable coal seams. The maximum thickness of a single seam reaches 6.5 m, with the cumulative thickness of all seams ranging from 1.2 to 23.6 m [28]. Specifically, the Taiyuan Formation encompasses 5 to 10 coal layers, with the 15th layer being the primary seam. In contrast, the Shanxi Formation includes three coal layers, with the No. 3 layer as its main seam (see Figure 1B). Both formations are rich in coalbed methane resources [28,31]. This paper focuses on the Panzhuang block, a key commercial area within the Qinshui Basin [27].

Hydrogeological drilling at the Sihe and Yonghong Mines in the Panzhuang block reveals that the No. 3 coal seam's maximum unit water inflow is 0.0122 L/(s·m), originating from the aquifer in the roof's sandstone fissures. The area's stable lithology and straightforward structure result in few faults and simplify the hydrogeological conditions [28,31]. The top and bottom of the 3# coal seam in the Panzhuang block consist of dense and low-permeability mudstone of significant thickness. This mudstone effectively blocks the hydraulic connectivity between the Taiyuan formation, the Shanxi formation, and the groundwater. The composition of water in the Carboniferous aquifer is of a stable Na-HCO_3-Cl type, as shown in Figure 2 [31,33]. This closed hydrological system, characterized by limited interaction with external water sources, provides favorable conditions for studying the phase change of solid-liquid fluid composition. The No. 3 coal seam of the Shanxi Formation is microscopically composed of 45–70% vitrinite, 20–36% inertinite, and 10–19% liptinite [28,31]. The No. 3 coal seam in the Shanxi Formation comprises 45–70% vitrinite, 20–36% inertinite, and 10–19% chitin. This coal exhibits a high degree of thermal evolution, with vitrinite reflectance ($R_{o,\,max}$) ranging from 2.79% to 3.98%. It has a gas content of 17.1 to 25.29 m^3/t and a gas saturation exceeding 90%. The coalbed methane (CBM) content in

the No. 3 coal seam varies from 0 to 35.57 m^3/t, typically ranging between 7 and 26 m^3/t. The seam thickness is generally between 5.0 and 7.0 m, and it is buried at depths of 300 to 800 m, making it a primary source of CBM production in the Panzhuang block [30,31].

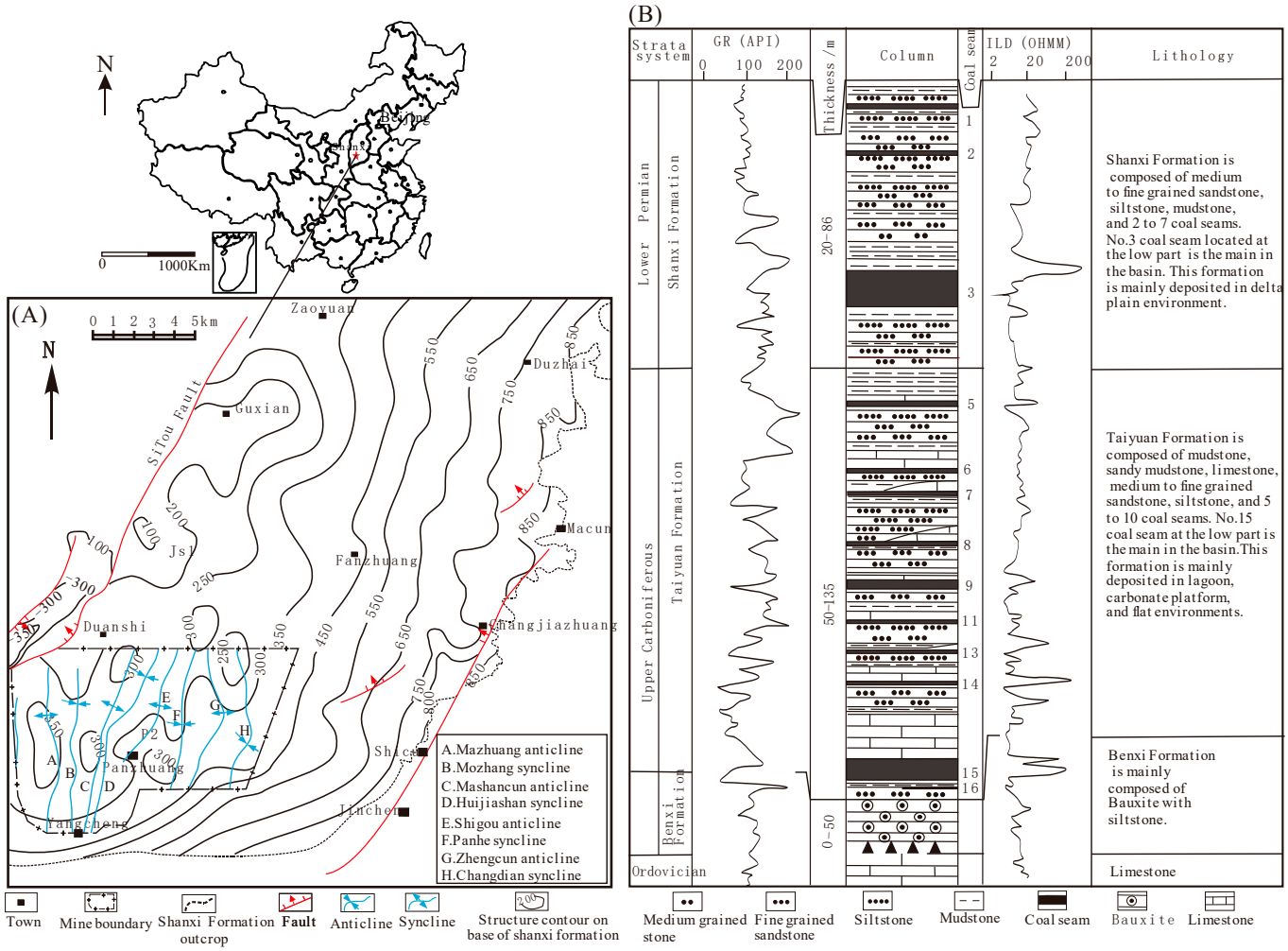

Figure 1. Structural location (**A**) and histogram (**B**) of southeastern Qinshui Basin [28,31,33].

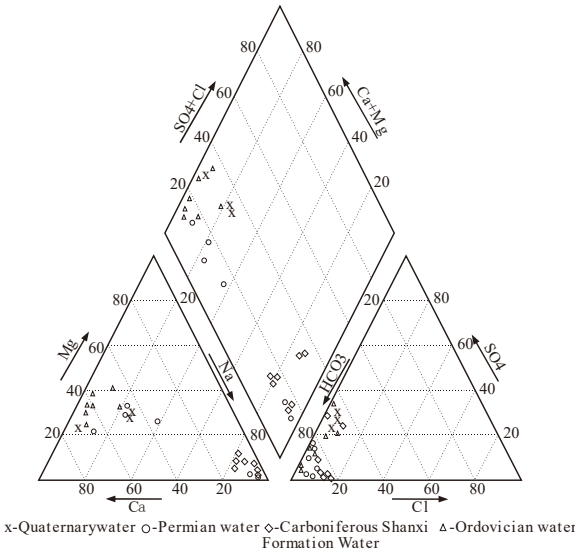

Figure 2. The piper of water composition types of different aquifers in Panzhuang block [19,31,33].

3. Experiments

3.1. Sampling Method

The sampling interval was set at 30 days, with five time points for each well both before and after the workover: 15 days, 45 days, 75 days, 105 days, and 135 days. Water samples were collected from the port of the tee joint of the production tree. In accordance with the 'Technical Regulation of Water Composition Sampling' (SL187-96) [34], polyethylene bottles were used as water containers. Each bottle was rinsed more than five times with the sampling water before being filled, sealed, and sent to the laboratory. To ensure comparability among the CBM wells, the research wells had to meet the following criteria:

(1) Water samples must be uniformly collected from coalbed methane production wells in the No. 3 coal seam in the Panzhuang block.
(2) The sampling wells should be located in coal seams with simple structures and wings in folds with similar dip angles.
(3) CBM wells must have a production history of more than 100 days, ensuring that the well is in the gas-water two-phase flow drainage stage, which helps to mitigate the impact of water environment changes caused by drilling and fracturing projects.

3.2. Experimental Method

The primary analysis process is as follows. First, the collected water samples are sent to the laboratory. Second, the water samples are left to stand at a room temperature of 30 °C for 24 h to allow for precipitation and stratification. Third, the mineral components of the upper and lower stratified samples are analyzed separately.

3.2.1. Analysis of Dissolved Minerals

Following the "Groundwater Composition Inspection Method (DZ/T0064-93)" [35], the water samples were analyzed for physical and chemical parameters, including K^+, Na^+, Ca^{2+}, Mg^{2+}, HCO_3^-, SO_4^{2-}, Cl^-, and PH. The instrument used in this experiment was an IC-2800 ion chromatograph. The specific experimental parameters were set as follows: the flow rate was 2 mL/min, the oven temperature was 30 °C, and the injection volume was 1 μL.

3.2.2. Characteristic Analysis of Sedimentary Minerals

Water samples from CBM wells were left for sedimentation and stratification. The sediment was then filtered and air-dried to obtain pulverized coal samples for testing and analysis of microscopic components and inorganic mineral components. For mineral composition analysis, a Rigaku D/max-2500 PC (made in Rigaku Corporation, Tokyo, Japan) fully automatic powder X-ray diffractometer was used to test the inorganic mineral composition of the pulverized coal samples. It should be noted that the GC-10 sediments were knocked over during transportation, causing contamination, and were therefore excluded from analysis.

4. Results

4.1. Dissolved Mineral Analysis Results

The dissolved minerals are presented in Table 1. The produced water from CBM wells contains the highest concentrations of Na^+, Cl^-, and HCO_3^-, while Ca^{2+}, Mg^{2+}, SO_4^{2-}, and other ions are present in smaller amounts. Each ion exhibits varying degrees of change before and after the workover (Figures 3–6).

Stable Drainage and Production Stage Before Workover (45 Days and Above): Ion concentrations remain relatively stable, with occasional fluctuations, but the overall trend is consistent. HCO_3^- ions increase slowly, while Cl^-, Na^+, and K^+ ions also show a gradual rise. Trace ions such as Ca^{2+} and SO_4^{2-} exhibit slight fluctuations, but these changes are minimal. The salinity of the produced water is relatively high, with a slight overall decrease.

Table 1. Analysis results of water samples at different time points before and after workover in CBM wells (unit in mg/L).

Well ID	Ions and Time	−135 Days	−105 Days	−75 Days	−45 Days	−15 Days	+15 Days	+45 Days	+75 Days	+105 Days	+135 Days
GC-06	Na^+	712.10	692.30	709.40	675.00	739.00	1056.90	802.30	730.20	605.90	542.60
	Mg^{2+}	12.41	12.04	11.23	12.31	13.25	29.52	16.30	11.35	10.92	11.96
	Ca^{2+}	14.63	13.21	14.32	13.24	21.50	42.45	32.61	19.32	13.46	13.85
	Cl^-	705.30	706.20	685.70	678.90	782.10	1042.30	843.20	679.50	680.60	673.80
	SO_4^{2-}	22.67	21.36	25.41	25.39	31.63	51.31	29.30	24.39	21.36	20.97
	HCO_3^-	582.30	578.40	599.30	601.97	621.60	421.22	580.32	633.40	708.40	729.50
	TDS	1702.30	1681.50	1678.20	1772.00	1982.00	2563.40	2346.20	1682.50	1681.50	1692.10
GC-09	Na^+	1026.90	1037.20	1007.10	987.70	1045.30	1555.20	1042.99	975.26	977.67	935.98
	Mg^{2+}	35.23	39.12	42.35	41.94	54.93	51.38	21.19	14.76	14.20	15.55
	Ca^{2+}	29.34	27.66	28.53	30.96	41.23	55.21	35.89	18.62	17.50	18.21
	Cl^-	392.40	370.60	372.50	351.20	373.00	854.99	766.16	583.35	404.78	375.94
	SO_4^{2-}	101.20	96.30	97.40	102.30	110.96	136.70	95.23	79.27	69.42	68.15
	HCO_3^-	1601.60	1642.90	1685.60	1633.50	1732.00	1406.85	1592.63	1665.16	1693.46	1703.05
	TDS	2674.50	2596.70	2545.70	2624.50	2822.00	3332.42	2631.20	2479.30	2496.70	2501.90
GC-10	Na^+	1152.86	839.67	752.96	648.51	616.08	1456.26	297.54	279.65	236.52	197.18
	Mg^{2+}	9.06	7.82	6.75	6.48	6.61	10.41	6.43	6.02	5.96	5.94
	Ca^{2+}	24.08	21.02	20.96	19.53	19.73	31.25	18.45	18.12	18.02	18.69
	Cl^-	905.59	580.66	490.35	407.98	416.14	1186.56	264.48	175.34	198.36	210.78
	SO_4^{2-}	24.65	23.65	22.65	21.16	21.37	32.05	17.98	18.16	18.25	18.28
	HCO_3^-	1665.35	1635.69	1662.25	1690.05	1673.15	1342.75	1712.85	1721.30	1728.56	1736.60
	TDS	3011.50	2503.74	2102.45	1989.30	1991.29	3210.63	1492.45	1451.33	1406.96	1349.00

GC-06 has a normal drainage history of 200 days, GC-09 is 150 days, and GC-10 is 120 days; "−" means before workover; "+" means after workover.

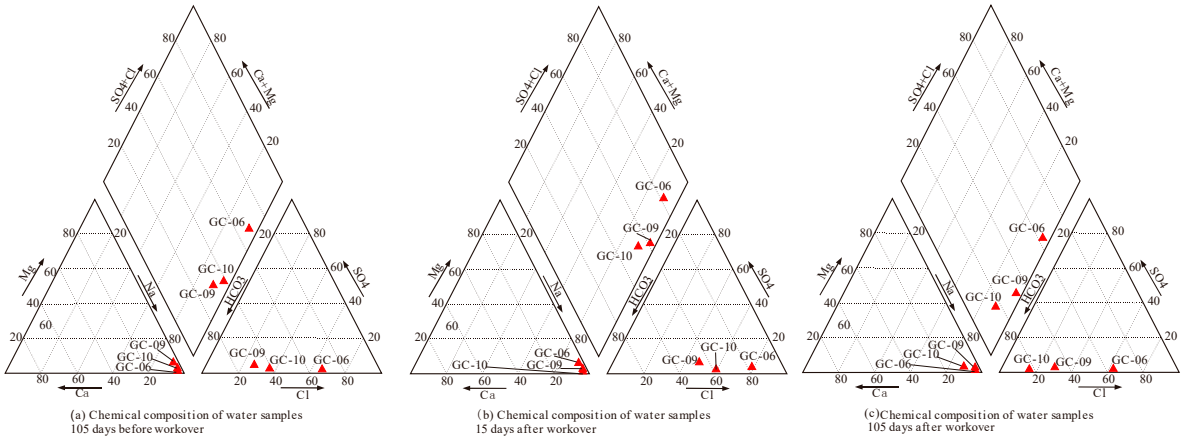

Figure 3. The piper of chemical composition of water samples from three CBM wells before and after workover. The water composition type in the stable production stage before and after the workover of 105 days: GC-06 is Na-Cl-HCO_3, and GC-09 and GC-10 are the Na-HCO_3-Cl type; the water quality type in the disturbance stage after the workover of 15 days: GC-06 is Na-Cl, and GC-09 and GC-10 are Na-Cl-HCO_3.

Disturbance Stage Before and After Workover (15 Days Before and After): Ion concentrations increase significantly before and after the workover, particularly for Na^+, Ca^{2+}, and Mg^{2+}. Compared to 45 days before the workover, the ion concentration changes are smaller in the 15 days prior to the workover. Among the three wells (GC-06, GC-09, and GC-10), the largest increase in Na^+ was observed in well GC-06 (64 mg/L), and the largest increase in Mg^{2+} was in well GC-09 (13 mg/L). However, the concentrations of Na^+ and Ca^{2+} in well GC-10 decreased. In the 15 days following the workover, ion concentrations

show significant changes. For example, Na^+ in well GC-10 increased by 840 mg/L, with other ions also showing substantial changes. Detailed changes are listed in Table 1.

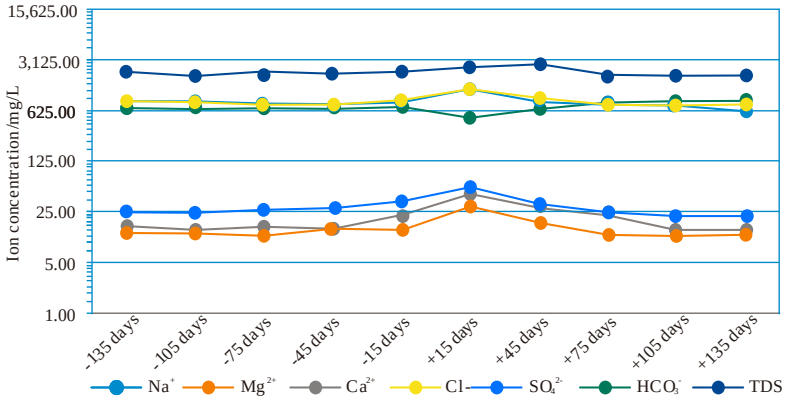

Figure 4. Phase changes of ions in water samples before and after workover of GC-06 well.

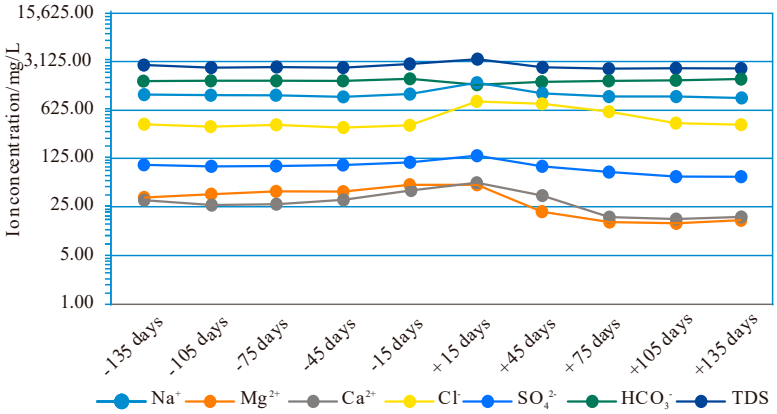

Figure 5. Phase changes of ions in water samples before and after workover of GC-09 well.

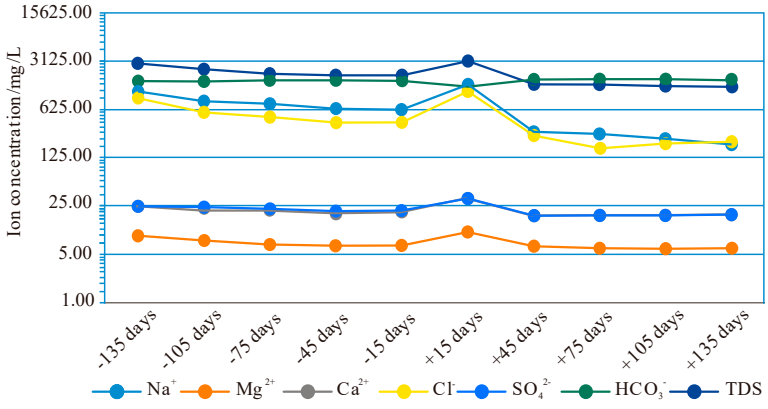

Figure 6. Phase changes of ions in water samples before and after workover of GC-10 well.

Stable Discharge and Production Stage After Workover (After 45 Days): Following the workover, ion concentration changes tend to stabilize, but the overall trend is a decline (Table 1 and Figures 4–6). In all three wells, Na^+, Cl^-, and Ca^{2+} concentrations gradually decrease, with the most significant reductions observed in Na+ and Cl^- ions.

4.2. Analysis Results of Precipitated Minerals

From the results shown in Table 2 and Figures 7 and 8, the output components of precipitated minerals in the water samples also have stage characteristics:

Table 2. The percentage of microscopic composition of precipitated minerals (in %).

Well ID	Time (Day)	Kaolinite	Illite	Chlorite	Illite/Smectite	Non-Clay Minerals	Vitrinite	Inertnite
GC-06	−45 days	16.74	10.65	3.80	6.85	2.86	36.50	22.60
	+15 days	8.59	5.47	1.95	3.52	1.47	60.20	18.80
	+45 days	17.28	11.00	3.93	7.07	2.96	42.53	15.23
GC-09	−45 days	13.79	11.49	4.21	8.81	0.00	40.10	21.60
	+15 days	8.75	7.29	2.67	5.59	0.00	59.20	16.50
	+45 days	15.27	12.73	4.67	9.76	0.00	42.24	15.34

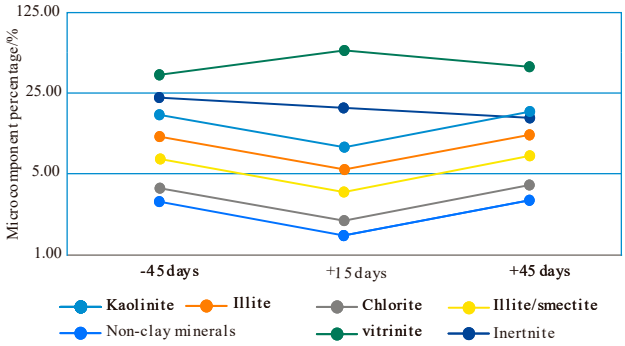

Figure 7. Compositional changes of precipitation minerals in Well GC-06 before and after workover.

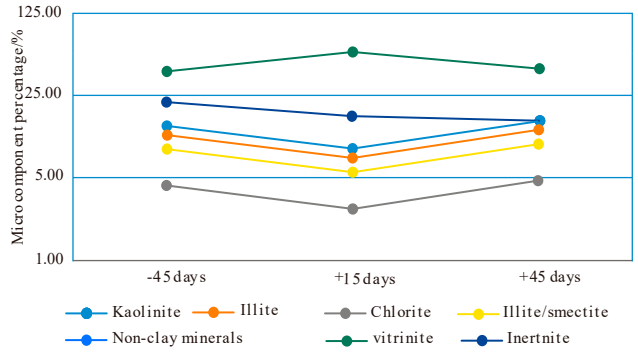

Figure 8. Compositional changes of precipitation minerals in Well GC-09 before and after workover.

Stable Drainage Period before Well Workover (prior to 15 days): During this period, the CBM-produced water showed the highest content of inorganic minerals within the precipitation minerals, reaching 40.9%. This was followed by vitrinite and inertinite, with the plastid group content at 36.5% and the inert group content at 22.6%. Among the inorganic minerals, clay minerals constituted the largest proportion. Specifically, clay minerals accounted for 93% of the inorganic component in well GC-06, and 100% in well GC-09. Kaolinite and illite were the predominant clay minerals in both wells, making up 16.74% and 10.65% of the microscopic composition, respectively.

Disturbed Drainage Period after Workover (within 15 days): During this time, the composition of precipitation minerals in the CBM-produced water changed significantly, with a notable decrease in the inorganic mineral content of the microscopic components. In well GC-06, the proportion of inorganic minerals dropped to 21%, and in well GC-09, it decreased to 24.3%. The microscopic composition also showed changes after the workover: vitrinite content increased while inertinite content decreased. For instance, in well GC-06, the vitrinite proportion increased by 23.7%, whereas the inertinite proportion decreased by 3.8% within 15 days post-workover compared to the initial 45 days.

During the stable drainage stage following the workover (after 45 days), the proportion of precipitated minerals essentially returned to pre-workover levels. Using GC-06 as an example, specific changes over the 45-day period before and after the workover were observed as follows: kaolinite increased from 16.7% to 17.28%, illite from 10.65% to 11.0%, chlorite from 3.8% to 3.93%, and vitrinite from 36.5% to 42.53%, and inertinite decreased from 22.6% to 15.23%. Detailed data can be found in Table 2.

5. Discussion

5.1. Analysis of Phase Change of Dissolved Minerals

The phase change of dissolved minerals results from chemical reactions triggered by the workover process. CBM workover operations necessitate sand flushing, requiring substantial quantities of workover fluids [36,37]. Regardless of how scientifically formulated the workover fluid ratio is, it will differ from the water composition within the coal reservoir. Additionally, to prevent damage to the coal reservoir, inhibitors and lubricants are often added to the workover fluids, further increasing the compositional difference between the workover fluids and the original water in the coal reservoir [23,37]. Consequently, the workover process induces a phase change in the dissolved minerals in the CBM well's output fluid. To analyze this phase change, this paper employs the Stiff diagram method [38], a hydrogeological technique for representing water composition, demonstrating that water compositions of samples from different sources—and even within the same source—can vary.

Figure 9, which is based on the concentration of anions and cations in the water samples, shows that before and after the workover, the stiff diagram exhibits a triangular or inverted flag-shaped map. This represents the gas-water two-phase flow stage [38,39], indicating that the water composition is dominated by Na^+, Cl^-, and HCO_3^- ions. Table 1 and Figures 4–6 also demonstrate that the dissolved mineral ions in the stable production stage are predominantly Na^+, Cl^-, and HCO_3^-, with trace ions such as Ca^{2+} and Mg^{2+} being less prevalent in the disturbance stage, both before and after the workover.

During the stable production stage, before and after the workover, the water composition types for the three CBM research wells were GC-06 (Na-Cl-HCO_3 type) as well as GC-09 and GC-10 (Na-HCO_3-Cl type). As shown in Figure 9, the ion composition in the stable production stage closely resembles that of the background ions in the No. 3 coal seam of the Shanxi Formation (Figure 2) [33,38].

Furthermore, the water composition type during the stable drainage stage suggests that the water in the No. 3 coal seam of the Shanxi Formation is not connected to the upper and lower water-bearing systems. This is because the surface water composition type is HCO_3-Ca, with Ca^{2+} as the main cation, contrasting with the Na^+ dominant water samples [33]. Therefore, there is minimal connection between surface water and the produced water in this area. In the Panzhuang block, surface river recharge is not the primary groundwater source, indicating a low degree of connectivity between different hydraulic systems. Consequently, the water composition changes before and after workovers can reveal the internal structural characteristics of coal reservoirs.

During the disturbance drainage stages before and after the workover, ion concentrations exhibited sharp changes compared to the stable production stage. Figures 3 and 9 illustrate that the water composition type GC-06 shifted from Na-Cl-HCO_3 to Na-Cl. Similarly, GC-09 and GC-10 transitioned from Na-HCO_3-Cl to Na-Cl-HCO_3, with the stiff diagrams showing a nearly funnel shape.

Before the workover, disturbances caused by drainage and production system failures led to pulverized accumulation in the wellbore, significantly increasing the ion concentration in the CBM wellbore water. This is well demonstrated by the rapid rise in TDS shown in Figures 4–6.

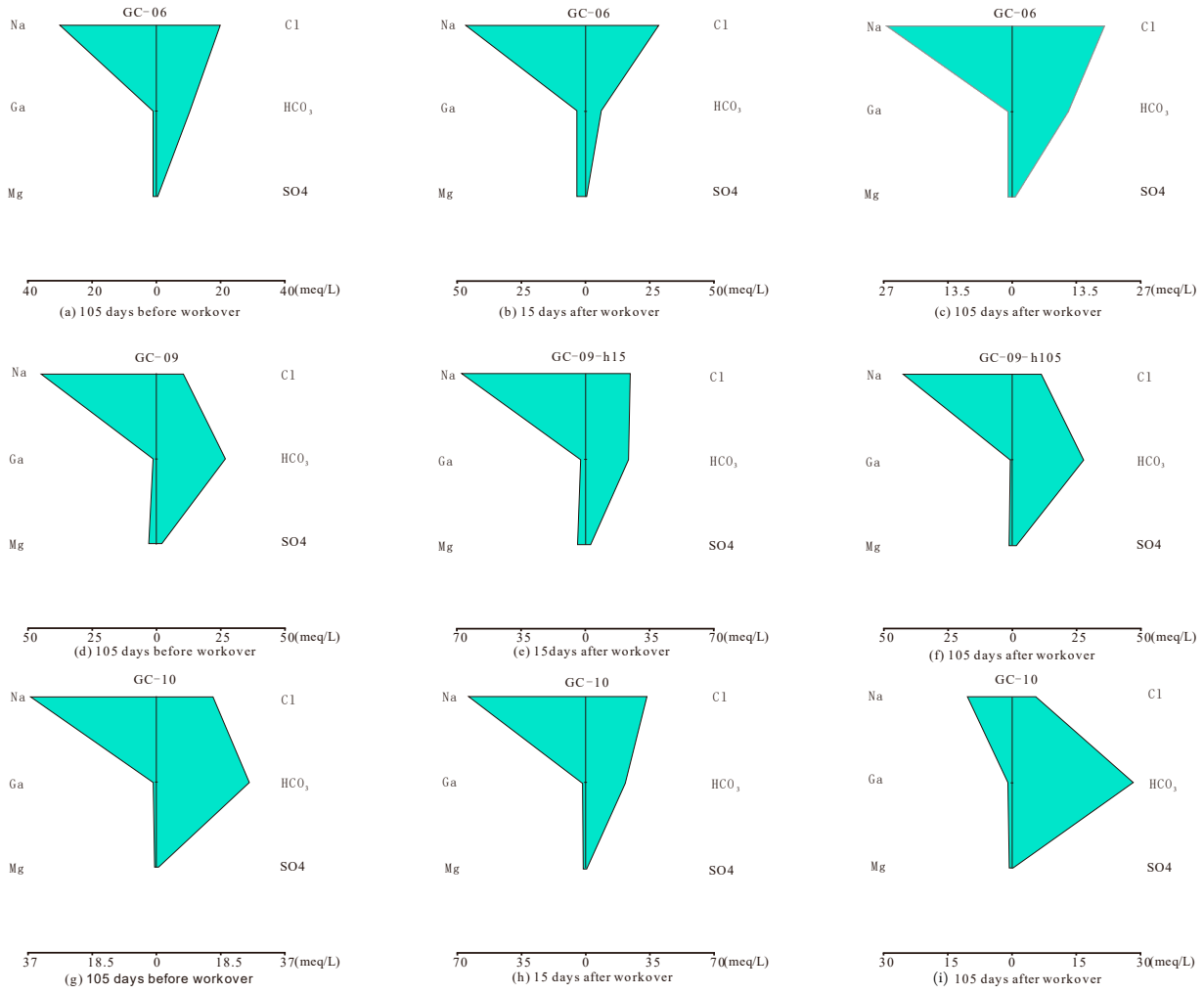

Figure 9. The stiff of water samples before and after workover in three wells.

After the workover, the concentrations of ions K^+, Na^+, Cl^-, and TDS surged, indicating that the workover fluid had contaminated the coal reservoir, drastically altering the ion concentration in the produced water [10,23]. This contamination is attributed to two main factors: Firstly, the workover fluid, rich in K^+ and Cl^- ions [10], increases the relative concentrations of Na^+ and Cl^- at certain stages post-workover, thereby polluting the coal reservoir (in Figure 9b,e,h). Secondly, coal seams contain abundant clay minerals, which, due to their large specific surface area, easily migrate and diffuse compared to other minerals [19,23]. Upon encountering water, these clay minerals dissolve or expand, altering the mineral composition of the produced fluid from CBM wells.

Additionally, the liquid used in the workover process differs from the coal reservoir water, leading to chemical reactions between the liquid components, further changing the ion composition of the produced water from CBM wells. For example, low-salinity surface water entering the coal seam can leach inorganic chlorine from the coal seam, altering the ion concentration.

5.2. Analysis of Stage Changes of Precipitation Minerals

In Figures 7 and 8, the composition of precipitated minerals in the produced fluid from the CBM well changed significantly before and after the workover. This indicates that the workover operation caused physical damage to the coal reservoir. The physical damage originated from the pressure disturbances due to the sand flushing operation and the frequent switching of the well during the workover [37]. It is well established that coal, a macromolecular mixture of inorganic and organic minerals [40], has a low

Young's modulus and high Poisson's ratio, making it particularly susceptible to physical damage when subjected to external forces [28]. Additionally, the lower part of the coal seam in the Qinshui Basin contains a certain proportion of tectonic coal, which is loose and fragmented [28,31]. As noted, the sand flushing operation during the workover is a primary factor in causing physical damage to the coal reservoir.

The intense impact force generated by the sand flushing operation fractured the original coal reservoir, with some of the resulting debris migrating into the wellbore along with the CBM-produced water. Table 2 and Figures 6 and 8 all demonstrate that post-workover, the proportion of vitrinite in GC-06 and GC-09 increased sharply among the precipitated minerals, primarily due to the sand flushing operation. Given that vitrinite is more brittle and easier to break than inertinite [41,42], and due to its lower density and higher mobility [42], the mineral composition of the precipitated minerals evolved over the different stages. The workover operation also caused an increase in bottom hole pressure, which deformed the coal skeleton and generated a certain amount of pulverized coal [43], further altering the composition of precipitated minerals.

This procedure promoted significant changes in the material composition, particularly in the presence of pulverized coal derived from the minerals within the coal matrix itself [28], which flowed out with the water produced by the CBM wells [43]. During the normal drainage and production stage, the process of steady-state drainage and pressure reduction helps avoid major damage to the coal reservoir. In this stable production stage, the fluid's carrying capacity in the coal reservoir is weak; thus, only fine-grained materials, mainly clay minerals due to their small grain size, are carried out [28]. Prior to the workover, during the stable production phase, the sediment in the produced fluids primarily consisted of inorganic minerals, with relatively little vitrinite and inertinite.

The particle size characteristics of pulverized coal changed throughout different mining stages. In the initial stage, most pulverized coal was produced mechanically, resulting in larger particles, with a microscopic composition similar to the original coal seam. During the early to middle stage, tectonic coal became the primary source of pulverized coal, causing only slight changes in its microscopic composition, and a slight increase in mineral content was observed. In the middle to late stage, the discharge of water and gas disrupted the equilibrium of stresses within the coal reservoir, leading to the mobilization of clay minerals from the coal skeleton by water, which increased the clay mineral content in pulverized coal. In the final stage, most pulverized coal, originating from tectonic coal, was expelled, with clay minerals mainly derived from those in the coal skeleton [28,44].

5.3. Mechanism Analysis of Influence on Gas Production Efficiency

While workover operations are essential for maintaining the normal function of CBM wells, improper conduct can significantly reduce their service life and gas production capacity (Figure 10 and Table 3). Post-workover, the ionic environment rapidly reverted to its pre-workover state, indicating a minimal impact on the reservoir. The degree of influence from workover operations on the reservoir was characterized by the mean square error (MSE) of ion concentrations over a period following the workover. A higher MSE indicates less ionic contamination and a reduced chemical impact on the reservoir. Thus, does the MSE affect gas and water production? The answer is affirmative. Analyzing the MSE data for ions from 15 to 105 days post-workover across three wells (Table 3), the variance in TDS, Na^+, and Cl^- levels indicated the extent of reservoir contamination. In particular, GC-10 displayed the largest changes in TDS, Na^+, and Cl^- among the three wells, suggesting minimal chemical pollution. Moreover, the ratios of daily gas and water production 105 days post-workover to those 105 days pre-workover demonstrate that GC-10 achieved the best recovery rates in both categories among the studied wells.

Table 3. The relationship between the mean square error of ions and the water/gas production of CBM wells after workover.

Well ID	Ions and Time	Mean Square Error of Each Ion from 15 to 105 Days after Workover	The Ratio of Daily Gas Production between 105 Days after Workover and 105 Days before Workover (%)	The Ratio of Daily Water Production between 105 after Workover and 105 Days before Workover (%)
GC-06	Na^+	171.64	76	80
	Mg^{2+}	9.39		
	Ca^{2+}	11.61		
	Cl^-	181.69		
	SO_4^{2-}	14.34		
	HCO_3^-	110.42		
	TDS	458.92		
GC-09	Na^+	317.09	86	82
	Mg^{2+}	19.55		
	Ca^{2+}	18.31		
	Cl^-	138.50		
	SO_4^{2-}	29.65		
	HCO_3^-	133.22		
	TDS	455.08		
GC-10	Na^+	674.21	93.2	92
	Mg^{2+}	2.42		
	Ca^{2+}	7.49		
	Cl^-	559.87		
	SO_4^{2-}	8.07		
	HCO_3^-	216.16		
	TDS	1004.07		

Figures 4–9 illustrate that the composition of the produced fluids from CBM wells altered significantly before and after the workover operation. This suggests that frequent flushing and switching of wells during these operations prompted changes in the internal structure of the coal reservoir. Coal, comprising both organic macromolecules and inorganic minerals, is susceptible to depressurization damage [10,28,45], making the deep coal seam prone to compound damage. This damage increases interactions between solid-phase particles and the coal and rock, thereby reducing the effective permeability of the coal seam [28,37]. The sand-washing operation generated a considerable impact force, causing the coal body to break and produce fine particles or pulverized coal. Additionally, the existing pulverized coal migrated within the fissure channels of the coal reservoir, potentially blocking these channels and further reducing permeability [23,37,45].

The introduction of new liquid components, due to the differing compositions of the workover fluid and the native liquids in the coal reservoir, inevitably leads to reactions between minerals like clay and water. If clay migration and expansion occur within the reservoir channels, they can cause blockage and consequent reservoir damage. Furthermore, frequent workover operations induce significant pressure differences, with the resulting shock waves agitating pulverized coal within the seam, leading to pressure-sensitive and velocity-sensitive effects. Such events can cause irreversible damage to the permeability of the coal reservoir [20,23,43].

Moreover, secondary migration of previously stable pulverized coal towards the wellbore [28], if not adequately discharged, can block channels and further decrease permeability. The reactions from migrated pulverized coal and pressure sensitivity also result in rougher coal cleavage surfaces, impairing fluid transport efficiency. Post-workover, equipment such as rod tube pumps influence the flow direction of the formation and wellbore liquids, with reverse fluid flow exacerbating damage to the coal reservoir [10,46]. This study observed changes in the material composition phases of the produced liquid from CBM wells pre- and post-workover, revealing transformations in the microstructure

of the coal reservoir. Future research should focus on leveraging these structural changes to achieve a positive transformation of the coal reservoir during workover operations.

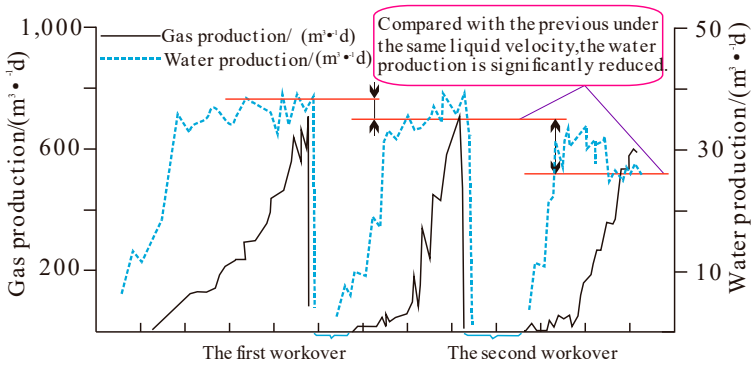

Figure 10. The workover operations of the CBM well reduced production efficiency [46].

6. Conclusions

The authors analyzed the output components from three CBM wells before and after workover operations. The findings indicate that workover operations cause both physical and chemical damage to the coal reservoir, leading to decreased gas and water production efficiencies. During the workover process, it is crucial to protect coal reservoirs and to choose the optimal timing for such operations. Additionally, this paper introduces a novel method of examining changes in output composition before and after workover to investigate the internal structure of coal reservoirs, which has been demonstrated to be scientifically viable. The authors anticipate that the results will guide future CBM production efforts. However, coal's complex internal structure, comprised of a mixture of macromolecular organic and inorganic matter, results in intricate damage mechanisms during workover processes, necessitating further investigation.

Author Contributions: Q.W.: writing—review and editing, writing—original draft, visualization, project administration, funding acquisition, conceptualization. Q.Y.: investigation, methodology, supervision, writing—review and editing, funding acquisition. Y.Z.: writing—review and editing, methodology, investigation. X.X.: writing—review and editing, investigation. C.H.: writing—review and editing. All authors have read and agreed to the published version of the manuscript.

Funding: This study is funded by the Geology and Mineral Resources Survey Project (No. DD20230563, Research on China's Energy Security Against the Background of International Carbon Reduction and New Geopolitical Patterns), the Basic Science Center Project for National Natural Science Foundation of China (No. 72088101, The Theory and Application of Resource and Environment Management in the Digital Economy Era), and the General Project of Henan Natural Science Foundation (242300421368).

Institutional Review Board Statement: Not applicable.

Informed Consent Statement: Not applicable.

Data Availability Statement: All data included in this study are available upon request by contact with the corresponding author.

Conflicts of Interest: The authors declare no competing financial interests.

References

1. Ministry of Natural Resources of China. National Oil and Gas Resources Exploration and Exploitation Bulletin (2020) [EB/OL]. Available online: http://gi.mnr.gov.cn/202109/t20210918_2681270.html (accessed on 18 September 2021).
2. Wang, H.; Liu, C. Process parameters design method of drainage gas recovery technology in gas-driven pump for coalbed methane production. *J. Pet. Sci. Eng.* **2019**, *207*, 109–167.
3. Li, S.; Tang, D.; Pan, Z.; Xu, H.; Tao, S.; Liu, Y.; Ren, P. Geological conditions of deep coalbed methane in the eastern margin of the Ordos Basin, China: Implications for coalbed methane development. *J. Nat. Gas Sci. Eng.* **2018**, *5*, 392–402. [CrossRef]

4. Huang, F.S.; Kang, Y.L.; You, L.J.; Li, X.C.; You, Z.J. Massive fines detachment induced by moving gas-water interfaces during early stage two-phase flow in coalbed methane reservoirs. *Fuel* **2018**, *222*, 193–206. [CrossRef]
5. Bai, T.; Chen, Z.; Aminossadati, S.M.; Rufford, T.E.; Li, L. Experimental investigation on the impact of coal fines generation and migration on coal permeability. *J. Pet. Sci. Eng.* **2017**, *159*, 257–266. [CrossRef]
6. Sobczyk, J. A comparision of the influence of adsorbed gases on gas stresses leading to coal and gas outburst. *Fuel* **2014**, *115*, 288–294. [CrossRef]
7. Perera, M.; Ranjith, P. Effects of saturation medium and pressure on strength parameters of Latrobe Valley brown coal: Carbon dioxide, water and nitrogen saturations. *Energy* **2011**, *36*, 6941–6947. [CrossRef]
8. Kang, J.; Elsworth, D.; Fu, X.; Liang, S.; Chen, H. Influence of water on elastic deformation of coal and its control on permeability in coalbed methane production. *J. Pet. Sci. Eng.* **2022**, *208*, 109603. [CrossRef]
9. Wang, G.; Wu, J.; Xiong, D.; Zhang, Z.; Zhao, Y.; Guo, H. Fine stable controlling technologies of water drainage and gas production in the Panhe CBM Gas Field, southern Qinshui Basin. *Nat. Gas Ind.* **2011**, *5*, 31–34.
10. Zhang, R.; Shen, F. Discussion of drainage system after workover operation of coalbed methane wells. *China Acad. J. Electron. Publ. House Shanxi Coal* **2019**, *6*, 74–78+98.
11. Kaiser, W.R.; Swartz, T.E.; Hawkins, G.J. Hydrology of the Fruitland formation, san juan basin. In *Geologic and Hydrologic Controls on the Occurrence and Productivity of Coalbed Methane, Fruitland Formation, San Juan Basin 1991*; Gas Research Institute Topical Report GRI-91/0072; Gas Research Institute: Des Plaines, IL, USA, 1991; pp. 195–241.
12. Pashin, J.C. Hydrodynamics of coalbed methane reservoirs in the black warrior basin: Key to understanding reservoir performance and environmental issues. *Appl. Geochem.* **2007**, *22*, 2257–2272. [CrossRef]
13. Guo, C.; Qin, Y.; Wu, C.F.; Lu, L.L. Hydrogeological control and productivity modes of coalbed methane commingled production in multi-seam areas: A case study of the Bide-santang basin, western Guizhou, south China. *J. Pet. Sci. Eng.* **2020**, *189*, 107039. [CrossRef]
14. Scott, A.R. Hydrogeological factors affecting gas content distribution in coal beds. *Int. J. Coal Geol.* **2002**, *50*, 363–387. [CrossRef]
15. Bachu, S.; Michael, K. Possible controls of hydrogeological and stress regimes on the producibility of coalbed methane in Upper Cretaceous-Tertiary strata of the Alberta basin, Canada. *Am. Assoc. Pet. Geol. Bull.* **2003**, *87*, 1729–1754. [CrossRef]
16. Li, X.; Fu, X.H.; Ge, Y.Y.; Chang, X.X. Research on sequence stratigraphy, hydrogeological units and commingled drainage associated with coalbed methane production: A case study in Zhuzang syncline of Guizhou province, China. *Hydrogeol. J.* **2016**, *24*, 2172–2187. [CrossRef]
17. Lamarre, R.A. Hydrodynamic and stratigraphic controls for a large coalbed methane accumulation in Ferron coals of east-central Utah. *Int. J. Coal Geol.* **2003**, *56*, 97–110. [CrossRef]
18. Qin, S.; Tang, X.; Song, Y.; Wang, H. Distribution and fractionation mechanism of stable carbon isotope of coalbed methane. *Sci. China Earth Sci.* **2006**, *12*, 1252–1258. [CrossRef]
19. Chen, S.; Tao, S.; Tian, W.; Tang, D.; Zhang, B.; Liu, P. Hydrogeological control on the accumulation and production of coalbed methane in the Anze Block, southern Qinshui Basin, China. *J. Pet. Sci. Eng.* **2021**, *198*, 108–138. [CrossRef]
20. Zhang, S.H.; Tang, S.H.; Li, Z.C.; Pan, Z.J.; Shi, W. Study of hydrochemical characteristics of CBM co-produced water of the Shizhuangnan Block in the southern Qinshui Basin, China, on its implication of CBM development. *Int. J. Coal Geol.* **2016**, *159*, 169–182. [CrossRef]
21. Xian, B.A.; Liu, G.F.; Bi, Y.S.; Gao, D.L.; Wang, L.; Cao, Y.; Shi, B.; Zhang, Z.; Zhang, Z.; Tian, L.; et al. Coalbed methane recovery enhanced by screen pipe completion and jet flow washing of horizontal well double tubular strings. *J. Nat. Gas Sci. Eng.* **2022**, *99*, 104430. [CrossRef]
22. Su, X.B.; Wang, Q.; Song, J.X.; Chen, P.; Yao, S.; Hong, J.; Zhou, F. Experimental study of water blocking damage on coal. *J. Pet. Sci. Eng.* **2017**, *156*, 654–661. [CrossRef]
23. Wei, Y.C.; Li, C.; Cao, D.Y.; Cui, B.L.; Xiang, Y.X. Effect of pulverized coal dispersant on coal in the CBM well-washing technology. *J. China Coal Soc.* **2018**, *7*, 1951–1958.
24. Chen, M.Y.; Chen, X.Y.; Wang, L.; Tian, F.-C.; Yang, Y.-M.; Zhang, X.-J.; Yang, Y.-P. Water adsorption characteristic and its impact on pore structure and methane adsorption of various rank coals. In *Environmental Science and Pollution Research*; Springer: Berlin, Germany, 2022. [CrossRef]
25. Wu, C.C.; Yang, Z.B.; Qin, Y.; Chen, J.; Zhang, Z.; Li, Y. Characteristics of hydrogen and oxygen isotopes in produced water and productivity response of CBM wells in western Guizho. *Energy Fuels* **2018**, *32*, 11203–11211. [CrossRef]
26. Yang, Z.; Qin, Y.; Wu, C.; Qin, Z.; Li, G.; Li, C. Geochemical response of produced water in the CBM well group with multiple coal seams and its geological significance-A case study of the Songhe well group in Western Guizhou. *Int. J. Coal Geol.* **2019**, *207*, 39–51. [CrossRef]
27. Qin, Y.; Shen, J.; Shi, R. Strategic Value and Choice on Construction of CMG Industry in China. *J. China Coal Soc.* **2022**, *47*, 371–387. [CrossRef]
28. Wang, Q.W. The Output Mechanism and Control Factors of the Pulverized Coal in Panzhuang Area, Qinshui Basin. Ph.D. Thesis, China University of Mining and Technology, Beijing, China, 2013.
29. Cao, D.Y.; Guan, Y.B.; Zhang, J.L.; Wu, G.Q.; Wang, C.Y.; Qian, G.M. *The Structural Characteristic of the East of Qinshui Coal Field*; The Press of Chongqing University: Chongqing, China, 1996; pp. 72–76.

30. Liu, H.L.; Li, G.Z.; Wang, G.J.; Wang, B. *The Geological Characters and Development Prospect of the Coalbed Methane in Qinshui Basin*; Petroleum Engineering Industry: Beijing, China, 2008.
31. Zhang, S.A.; Hua, Z.J.; Zhang, P. *The Design Illustration of the Development of Panzhuang Coalbed Methane Project*; The Internal Report of Blue Flame Coalbed Methane: Jinchen, China, 2009.
32. Ye, J.P.; Wu, Q.; Ye, G.J.; Chen, C.L.; Yue, W.; Li, H.Z.; Zhai, Z.R. Study on the coalbed methane reservoir-forming dynamic mechanism in the southern Qinshui basin, Shanxi. *Geol. Rev.* **2002**, *3*, 319–323.
33. Zhang, X.M. Chemical Characteristics and Dynamic Field Analysis of CBM Produced Water in the Southern Qinshui Basin. Master's Thesis, Henan Polytechnic University, Jiaozuo, China, 2012.
34. *Chinese Industry Standard SL187-96*; Technical Regulation of Water Composition Sampling. Ministry of Water Resource of the People's Republic of China: Beijing, China, 1997.
35. *Chinese Industry Standard DZ/T 0064.1~0064.80-93*; Groundwater Composition Inspection Method. Ministry of Geology and Mineral Resources of the People's Republic of China: Beijing, China, 1993.
36. Pashin, J.C.; Pradhan, S.P.; Vishal, V. *Formation Damage in Coalbed Methane Recovery, Formation Damage during Improved Oil Recovery*; Gulf Professional Publishing: London, UK, 2018; pp. 499–514.
37. Mao, Z.Y. Study of Technology and Key Equipment Design Based on CBM Wells Workover Reservoir Protection. Master's Thesis, China University of Petroleum, Beijing, China, 2018.
38. Li, Z.C.; Tang, S.H.; Wang, X.F.; Zheng, G.Q.; Zhu, W.P.; Wang, S.S.; Zhang, J.P. Relationship between water chemical composition and production of coalbed methane wells, Qinshui basin. *J. China Univ. Min. Technol.* **2011**, *3*, 424–429.
39. Qin, Z.H. Microbial Community Evolution and Gas Water Interaction Mechanism in the Process of Producing Water from Coalbed Methane Wells. Master's Thesis, China University of Mining & Technology, Beijing, China, 2021.
40. Si, L.; Wei, J.; Xi, Y.; Wang, H.; Wen, Z.; Li, B.; Zhang, H. The influence of long-time water intrusion on the mineral and pore structure of coal. *Fuel* **2021**, *290*, 119848. [CrossRef]
41. Liu, H.; Huang, W.H.; Ao, W.H.; Lu, X.X.; Liu, S.P.; Luo, J.L. Controls of coal maceral composition of coal seam 3# and 15# on microfracture in south Qinshui basin. *Resour. Ind.* **2012**, *4*, 75–81.
42. Han, D.X.; Ren, D.Y.; Wang, Y.B.; Jin, K.L.; Mao, H.L.; Qin, Y. *Coal Petrology of China*; China University of Mining & Technology Press: Beijing, China, 1996; pp. 26–37.
43. Tao, S.; Tang, D.; Song, H.; Li, S. The influence of flow velocityon coal fines output and coal permeability in the Fukang Block, southern Junggar Basin, China. *Sci. Rep.* **2017**, *7*, 14–124. [CrossRef]
44. Cao, D.Y.; Yuan, Y.; Wei, Y.C.; Liu, S.G.; Li, X.M.; Wang, Q.W. Comprehensive classification study of coal fines genetic mechanism and origin site. *Coal Geol. China* **2012**, *1*, 10–12.
45. Wei, K.Q.; Liu, G.J.; Wang, X.D.; Ma, X.N.; Duan, J.; Chang, F.C. Conventional workover operation technology of coalbed methane. *Chem. Enterp. Manag.* **2020**, *16*, 196–197.
46. Wang, Q. Timeliness Analysis of Coalbed Methane Workover for Reducing Damage to Coal Reservoirs. *ACS Omega* **2022**, *8*, 6956–6962. [CrossRef] [PubMed]